Published in: Polymer (2005), vol. 46, iss. 6, pp. 1943-1948
Status: Postprint (Author's version)

Stretching calorimetry studies of poly(ε-caprolactone)/organoclay nanocomposites

Vitaly M. Karaman[a], Eleonora G. Privalko[a], Valery P. Privalko[a], Dana Kubies[b], Rudolf Puffr[b,] and Robert Jérôme[c]

[a]Institute of Macromolecular Chemistry, National Academy of Sciences of Ukraine, 02160 Kyiv, Ukraine
[b]Institute of Macromolecular Chemistry, Academy of Sciences of the Czech Republic, Heyrovsky Sq. 2, 162 06 Prague, Czech Republic
[c]Center for Education and Research on Macromolecules (CERM), University of Liège, Sart-Tilman, B6, B-4000, Belgium

Abstract

Poly(ε-caprolactone)/montmorillonite nanocomposites, prepared by bulk ring-opening polymerization of ε-caprolactone in the presence of tin(II) 2-ethylhexanoate as a catalyst and hydroxy groups of ammonium tethers of organoclay acting as chain-growth centers, were characterized by the stretching calorimetry technique. In the range of elastic (reversible) deformations, experimental Young's moduli and linear thermal expansivities of both the intercalated and exfoliated nanocomposites could be fitted to the predictions of Chow's model assuming the apparent aspect ratio of clay nanoparticles of the order of 10. In the range of anelastic deformations, the values of the internal energy increments $\Delta U/m$ for the intercalated nanocomposite lay somewhat below those for the corresponding neat polymer, while the $\Delta U/m$ vs. ε plots for the exfoliated nanocomposite and for the corresponding neat polymer were nearly identical both in shape and in absolute values over the entire range of strains, up to the breaking strains ε_b. These data suggested higher and lower probabilities of interfacial debonding in the range of anelastic deformations for intercalated and exfoliated samples, respectively.

Keywords: Organoclay nanocompsites; Poly(ε-caprolactone); Stretching calorimetry

1. Introduction

Polymer-layered aluminosilicate nanocomposites (NC) proved to be exceptionally promising lightweight and easily processable engineering materials with high stiffness, strength, heat resistance, flame retardance and gas/liquid barrier properties [1-5]. The dispersion of 3–5 wt% of clay particles, delaminated to individual silicate platelets of 1 nm thick, improves properties of the nanocomposites to the same extent as 30–50 wt% of glass fibers or other micron-sized fillers. Owing to their large aspect ratio, the platelets start to interact forming 3D structure throughout the polymer matrix at a concentration of clay exceeding ~1 wt%.

To achieve such effect, it is necessary to modify (organophilize) particles of the original hydrophilic clay. This can be done, e.g. in water, by dispersing the clay to individual randomly distributed platelets (exfoliation) and neutralizing their negative charges with such organic cations which provide compatibility, or even chemical bonding [1, 6] to the polymer matrix. Dried particles of the modified organoclay (OC) represent an organic/inorganic intercalate consisting of stacks of silicate platelets separated by tethered organic cations forming the so called gallery.

Nanocomposites are prepared mostly by polymerization of the monomer-OC suspensions or by mixing the OC and the polymer in the molten state. Molecules of a monomer or a polymer penetrate into the galleries increasing interlayer distances. Depending on thermodynamic parameters, the process either stops at the stage of intercalate swollen by the polymer, keeping the silicate plates in parallel arrangement, or continues until a complete exfoliation is achieved [2-6].

The aim of this work was to gain a deeper insight into structure properties by thermoelastic characterization of poly(ε-caprolactone) nanocomposites with intercalated (NC-In) and exfoliated (NC-Ex) montmorillonite, using the stretching calorimetry method which has not been used for the purpose so far.

2. Experimental part

2.1. Materials

Organically modified clays were prepared by a standard cation-exchange reaction. The Na montmorillonite (Cloisite Na, Southern Clay Products, 0.92 mmol of Na^+/g) was modified with either diethyl(3-hydroxypropyl)octadecylammonium bromide (organoclay OC1) or with a 4:6 mol/mol mixture of dodecyl(dimethyl)octadecylammonium bromide and diethyl(3-hydroxypropyl) octadecylammonium bromide (organoclay OC2).

ε-Caprolactone (Fluka) was dried over calcium hydride at room temperature for 48 h and distilled under reduced pressure just before use.

2.2. Composite preparation

Poly(ε-caprolactone)/organoclay nanocomposites were prepared by bulk ring-opening polymerization of ε-caprolactone in the presence of tin(II) 2-ethylhexanoate as a catalyst and hydroxy groups of ammonium tethers acting as chain-growth centers. The montmorillonite content was determined by thermogravimetry, the structure of nanocomposites by WAXS and TEM. The molecular weight of poly(ε-caprolactone) released from the silicate by extraction with LiCl solution in THF was determined by the size exclusion chromatography [6]. The PCL homopolymers, PCL27 and PCL46, were a gift from CERM, University of Liège. Selected properties of studied samples are shown in Table 1.

Table 1. Selected properties of poly(ε-caprolactone) homopolymers and nanocomposites

Sample	$\langle M_n \rangle$[a]	Clay content[b] (wt%)	Clay dispersion[c]	Density (g/cm^3)	Young's modulus (GPa)	Linear expansivity (10^4 K^{-1})	ε^* (%)	ε_b (%)
PCL46[d]	46000	0	–	1.144	0.55±0.03	1.76±0.04	1.8±0.1	15.6
PCL27[d]	27000	0	–	1.086	0.52±0.03	2.10±0.05	1.5±0.1	4.1
NC-In[e]	27100	8.2	Intercalated	1.153	0.78±0.04	1.18±0.04	0.3±0.1	4.5
NC-Ex[f]	38400	3	Exfoliated	1.147	0.72±0.04	1.34±0.04	0.4±0.1	5.6

[a] Size exlusion chromatography, PCL recalibration.
[b] Thermogravimetrically.
[c] WAXS measurement.
[d] Poly(ε-caprolactone) homopolymer.
[e] PCL nanocomposite; the clay used for the polymerization was modified with a mixture of diethyl (3-hydroxypropyl)octadecylammonium) and dodecyl(dimethyl)octadecylammonium bromide (6:4 mol/mol).
[f] PCL nanocomposite; the clay used for the polymerization was modified with diethyl(3-hydroxypropyl)octadecylammonium bromide.

Polymer films (55×20×0.5 mm) for stretching calorimetry measurements were prepared by the melt pressing method. A required amount of the sample was dried in vacuum overnight and then placed in a metal form and melted at 120 °C in a press. The melt was degassed and pressed with force of 50 kN for 2 min followed by 100 kN for another 2 min; then it was cooled to 10 °C under pressure of 100 kN for 15 min.

2.3. Technique

The mechanical work (W) and concomitant heat effects (Q) in the stepwise loading (stretching)/unloading (contraction) cycles were measured (with the estimated mean error below 2%) at room temperature using a stretching calorimeter described in detail elsewhere [7-9]. In every experimental run, each specimen was stretched at a constant velocity q^+(10% of the total specimen length per minute) to a predetermined strain ε_i, stored at fixed ε_i to complete mechanical and thermal relaxations, and thereafter allowed to contract at the same velocity q^- to zero force [7]. The typical difference between fixed strains in two successive steps, $\varepsilon_{i+1}-\varepsilon_i$, varied

from several digits at fourth decimal place to a few digits at the third place within the strain intervals below and above 1.5%, respectively.

3. Results and discussion

3.1. Nanocomposite samples

The polymerization of ε-caprolactone initiated by the end hydroxy groups of ammonium cations attached to the inner silicate surface in OC galleries resulted in the tethered poly(ε-caprolactone) (PCL) chains onto the silicate platelets. The volume of galleries increases with the PCL molecular weight and beyond a certain value, which is $M_n \geq 15{,}000$ for our organoclay OC1, nanoparticles exfoliate [6]. The prepared nanocomposite NC-Ex with the molecular weight of the PCL matrix M_n=38,400 and the clay content 3 wt% did not exhibit interlamellar WAXS reflection and was considered as highly exfoliated.

With increasing OC loadings in nanocomposites, the final molecular weight of PCL decreases and beyond a certain value only the intercalated structure is obtained [6]. To prepare the nanocomposite with a higher loading of the clay and not too low M_n, the concentration of initiating hydroxy groups in OC2 was lowered to 60% of that of OC1. However, in spite of the high molecular weight of the PCL matrix (M_n 27 100), the resulting NC-In containing 8.2 wt% clay was only intercalated system with the interlamellar distance d_{001}=3.05 nm. Interestingly, the intercalated morphology was observed also in the case of in situ prepared PCL nanocomposite (M_n 35,500, 3 wt% of the clay) with Cloisite 25A containing only dodecyl(dimethyl)octadecylammonium tether with no initiating hydroxy groups [6]. The polymer molecular weight and the clay concentration were comparable with the values for the exfoliated nanocomposite NC-Ex. This example indicates that the intercalated structure of NC-In compared with the exfoliated one in NC-Ex stems neither from the different PCL molecular weight nor from the clay concentration, but most probably from the presence of dodecyl(dimethyl)octadecylammonium tether in the NC-In.

The primary role of alkylammonium tethers is to move silicate plates farther apart and thus to reduce their mutual cohesive forces. This role was played well by tethers both in OC1 and OC2 organoclays. The interlamellar distance d_{001} of the original montmorillonite (Cloisite Na) was shifted from 1.22 to 2.17 nm and to 2.36 nm for OC1 and OC2, respectively.

In the course of nanocomposite preparation from a relatively polar monomer or a polymer melt, the extent of layered silicate swelling and exfoliation is facilitated, according to the thermodynamic models [10-12], by maximizing the strength and number of favourable interactions between the polymer and the silicate surface while minimizing the strength and number of unfavorable interactions of the polymer with nonpolar alkyls of the tether. In case of our exfoliated nanocomposite NC-Ex, the contribution of attractive interactions to the Gibbs energy (interactions of the monomer and polymer segments with the silicate surface, ammonium, hydroxy or ester groups of the tether) obviously exceeds the contribution of repulsive interactions of the monomer and polymer with the tether alkyls.

However, the opposite situation occurs when the tether contains two long alkyls like in OC2. The average distance between sites in these organoclays based on Cloisite Na is calculated to be 1.16 nm assuming their distribution in a squared net on the surface area of 750 m^2/g. Two long tether alkyls with the diameters 0.4–0.5 nm sterically reduce the opportunity of polymer segments to interact with the silicate surface [10]. As a consequence of 40% substitution of 3-hydroxypropyl group for dodecyl in tethers of organoclay OC2, the number of attractive interactions between polymer and the silicate surface is reduced and the number of repulsive interactions of polymer with the long tether alkyls is increased, which leads to an intercalated structure of nanocomposite NC-In. On the other hand the 40% substitution of two ethyl groups in OC1 tethers for methyls in OC2 has a negligible influence on nanocomposite morphology.

3.2. Range of elastic (reversible) deformations

As can be seen from Fig. 1, in the range of elastic deformations below a certain characteristic limiting strain ε^*, the specific (per sample mass m) mechanical work (W/m) and specific heat effects (Q/m) data for all studied samples obeyed (dashed lines) the classic equations of the thermoelasticity of solids [7]

Published in: Polymer (2005), vol. 46, iss. 6, pp. 1943-1948
Status: Postprint (Author's version)

$$W/m=E\varepsilon^2/2\rho \tag{1a}$$

$$Q/m=E\alpha_L T\varepsilon/\rho \tag{1b}$$

(where E is Young's modulus, α_L is the linear thermal expansion coefficient and ρ is the density).

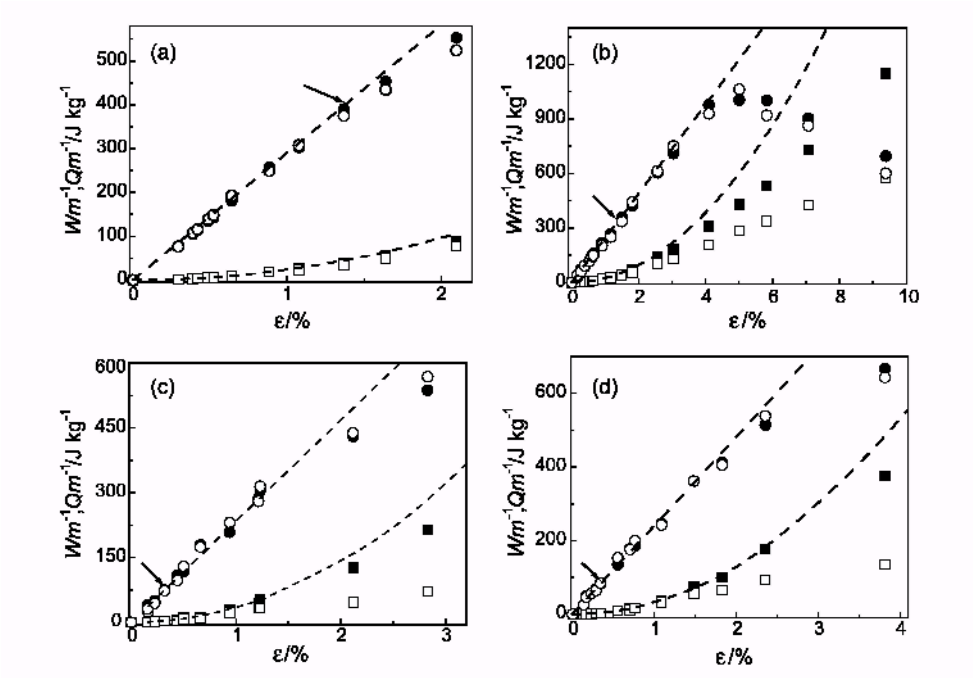

Fig. 1. Strain dependences of the specific mechanical work (squares) and specific heat effects (circles) in stretching (filled symbols)/contraction (open symbols) cycles for homopolymer PCL27 (a), homopolymer PCL46 (b), nanocomposite NC-In (c) and nanocomposite NC-Ex (d). Limiting strains (ε^* for elastic behaviour is indicated by arrow.

As expected, the best-fit values of E and α_L (Table 1) for both nanocomposites were significantly higher and lower, respectively, than those for the corresponding neat samples. This result is clearly a consequence of a much higher Young's modulus and of a much lower linear expansion coefficient of the clay compared with those for the neat polymers. It can be easily verified that the equations of Nielsen [13] Eq. (2) and of Wang and Kwei [14] Eq. (3) greatly underestimated and overestimated, respectively, the Young's modulus and the linear thermal expansivity of the intercalated nanocomposite NC-In whatever trial values of φ_{max} were.

$$\frac{E}{E_1}=\frac{1+AB\varphi}{1-BC\varphi} \tag{2}$$

$$\alpha_L=\alpha_{L,1}-\varphi(\alpha_{L,1}-\alpha_{L,2})\theta \tag{3}$$

where $A=(7-5\nu_1)/(8-10\nu_1)$; $B=(E_2-E_1)/(E_2+AE_1)$; $C=1+[(1-\varphi)/\varphi_{max}^2]\varphi$; $\theta=(3E_2/E_1)\varphi/(E_2/E_1)[2\varphi(1-2\nu_1)+(1+\nu_1)]+2(1-\varphi)(1-2\nu_2)$; ν_i's are Poisson's coefficients; φ_{max} is the maximum packing factor for filler particles, and subscripts 1 and 2 refer to the polymer matrix and the filler, respectively.

Even more striking differences were observed for the exfoliated sample NC-Ex (in calculations, $E_2\approx178$ GPa [15] and $\alpha_{L,2}\approx1\times10^{-6}$ K^{-1} [16], respectively, were assumed for the clay). There is little doubt that these glaring discrepancies should be attributed to the violation of the underlying assumptions of the above equations on the isometric (i.e., of the aspect ratio $l/d=1$) shape of filler particles [13-14]. For this reason, the experimental data were treated with the more appropriate relationships of Chow [17] for composites with uniaxially oriented, plate-like (i.e., of the aspect ratio $l/d\gg1$) particles,

Published in: Polymer (2005), vol. 46, iss. 6, pp. 1943-1948
Status: Postprint (Author's version)

$$\frac{E}{E_1} = 1 + \frac{(B_2/B_1 - 1)X_1 + 2(G_2/G_1 - 1)Y_1}{2Y_1X_3 + X_1Y_3}\varphi \tag{4}$$

$$\alpha_L = \alpha_{1L} + \frac{B_2}{B_1}\frac{(\alpha_{2V} - \alpha_{1V})\langle Y_1\rangle\varphi}{2\langle X_1\rangle\langle Y_3\rangle + \langle Y_1\rangle\langle X_3\rangle} \tag{5}$$

where B and G are the bulk and shear moduli, respectively, α_V is the effective volumetric thermal expansivity,

$$X_i = 1+(B_2/B_1-1)(1-\varphi)\alpha_i \tag{6a}$$

$$Y_i = 1+(G_2/G_1-1)(1-\varphi)\beta_i \tag{6b}$$

$$\langle X_i\rangle = 1+(B_2/B_1-1)[(1-\varphi)\alpha_i+\varphi] \tag{6c}$$

$$\langle Y_i\rangle = 1+(G_2/G_1-1)[(1-\varphi)\beta_i+\varphi] \tag{6d}$$

α_i and β_i (i=1,3) are the functions of the particle aspect ratio l/d and Poisson's ratio of the matrix (see the Appendix of the original paper [17] for relevant details).

As can be seen from Fig. 2, the experimental values of both the Young's modulus E and the linear expansivity $\alpha_{L,1}$ for the exfoliated sample NC-Ex nearly quantitatively fitted to the theoretical expressions Eqs. Figs. (4) and (5), respectively, assuming aspect ration l/d=10. The somewhat lower value derived from similar calculations for the intercalated nanocomposite NC-In seems reasonable because intercalated clay particles have lower aspect ratio compared to clay platelets. It would be pertinent to remark here, however, that the actual aspect ratio for clay platelets is higher than the 'effective' value reported above, in so far as in our calculations a perfect, longitudinally oriented structure of all nanoparticles was assumed.

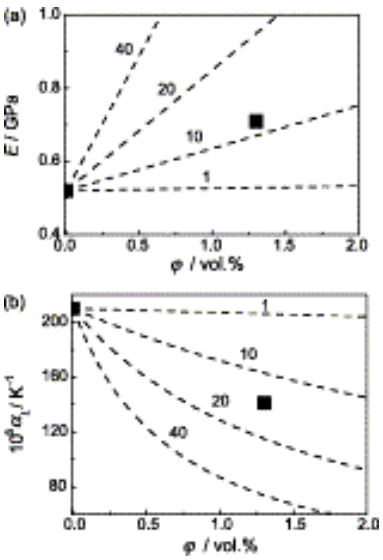

Fig. 2. Fits of the experimental values (▪) of Young's modulus (a) and of linear thermal expansivity (b) for the exfoliated sample NC-Ex to Eqs. Figs. (4) and (5). The numbers at theoretical curves refer to the assumed aspect ratio of clay nanoparticles. The estimated errors correspond, approximately, to the sizes of the data points.

3.3. Range of anelastic deformations

As can be seen from Fig. 1, the anelastic deformation of nanocomposites (manifesting itself by higher than double experimental-error difference between W/m and Q/m in stretching and contraction cycles, as well as by deviations of experimental data points from theoretical curves) sets on at somewhat smaller limiting strains ε^* compared with the neat polymer. In view of correlation between the limiting strain ε^* and the yield strain ε_y [18], it could be suggested that the observed depression of ε^* in nanocomposites was the result of debonding at the

nanoparticle-matrix interface [16]. In this case, the internal energy increments, $\Delta U/m=W/m+Q/m$, in the strain region above ε^* should have been significantly smaller in nanocomposites than in the neat polymer [16].

As can be seen from Fig. 3(a), the values of $\Delta U/m$ above ε^* for the intercalated nanocomposite NC-In in fact, lay somewhat below those for the corresponding neat polymer (PCL27), while the $\Delta U/m$ vs. ε plots for the exfoliated sample NC-Ex and for the corresponding neat polymer (PCL46) were nearly identical, both in shape and in absolute values, over the entire range of strains, up to the breaking strains ε_b (Fig. 3(b)). In terms of the $\Delta U/m$ criterion, these data suggest higher and lower probabilities of debonding in the range of anelastic deformations for intercalated and exfoliated samples, respectively.

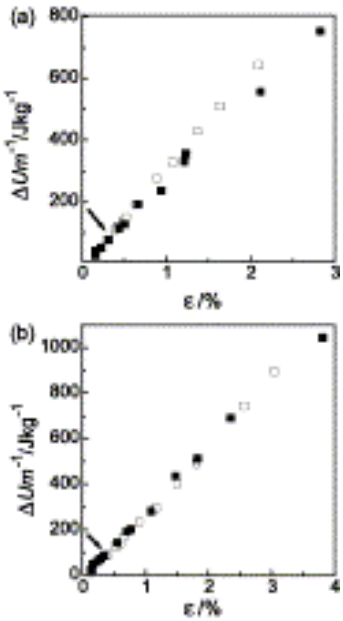

Fig. 3. Strain dependences of the specific internal energy increments in stretching for (a) homopolymer PCL27 (open squares) and nanocomposite NC-In (filled squares), and (b) homopolymer PCL46 (open squares) and the nanocomposite NC-Ex (filled squares). Limiting strain ε^* of nanocomposites is indicated by arrow.

Theoretically, all polymer molecules in our nanocomposites should be chemically bonded to the tethers via hydroxy groups. However, protic impurities, mostly water in clays, which could be hardly dehydrated, act as potential chain growth initiators, too. The higher is the concentration ratio clay/tether hydroxy groups, the higher fraction of PCL molecules not bonded to the silicate could be expected. The higher probability of interfacial debonding in the intercalate NC-In compared with exfoliated NC-Ex is most probably a consequence of both a higher fraction of PCL molecules not bonded to the silicate and a lower thermodynamic compatibility of PCL with organoclay OC2, as discussed in the Part 3.1.

4. Conclusions

In the range of elastic (reversible) deformations, experimental Young's moduli and linear thermal expansivities of both the intercalated and exfoliated nanocomposites could be fitted to the predictions of Chow's model [17] assuming the aspect ratio of clay nanoparticles of the order of 10.

In the range of anelastic deformations, the values of the internal energy increments $\Delta U/m$ for the intercalated nanocomposite lay somewhat below those for the corresponding neat polymer, while the $\Delta U/m$ vs. ε plots for the exfoliated sample and for the corresponding neat polymer were nearly identical, both in shape and in absolute values, over the entire range of strains, up to the breaking strains ε_b. These data suggested higher and lower probabilities of interfacial debonding in the range of anelastic deformations for intercalated and exfoliated samples, respectively.

Acknowledgements

D.K. and R.J. are much indebted to the 'Services généraux des affaires scientifiques, techniques et culturelles; coopération S&T avec l'Europe centrale et orientale (Bruxelles)' for support of CERM and a postdoctoral fellowship for D.K. Financial support by the Grand Agency of ASCR (grant No. KJB 4050309) is also gratefully acknowledged.

References

[1] Fukushima Y, Inagaki S. J Inclusion Phenom 1987;5:473-82.
[2] LeBaron PC, Wang Zhen, Pinnavaia TJ. Appl Clay Sci 1999;15: 11-29.
[3] Pinnavaia TJ, Beall GW. Polymer-clay nanocomposites. New York: Wiley; 2000.
[4] Alexandre M, Dubois Ph. Mater Sci Eng 2000;R28:1-68.
[5] Biswas M, Ray SS. Adv Polym Sci 2000;155:167-221.
[6] Kubies D, Pantoustier N, Dubois Ph, Rulmond A, Jérôme R. Macromolecules 2002;35:3318-20.
[7] Godovsky YuK. Thermal physics of polymers. Munich: Springer; 1991.
[8] Mirontsov LI. Thermodynamics of deformation of segmented polyurethanes. PhD Thesis, Institute of Macromolecular Chemistry, National Academy of Sciences of Ukraine, Kyiv, 1987.
[9] Sukhorukov DI. Thermodynamics of reversible and irreversible deformations at the uniaxial loading of filled polymers. PhD Thesis, Institute of Macromolecular Chemistry, National Academy of Sciences of Ukraine, Kyiv, 2001.
[10] Fornes TD, Hunter DL, Paul DR. Macromolecules 2004;37:1793-8.
[11] Vaia RA, Giannelis EP. Macromolecules 1997;30:7990-9.
[12] Vaia RA, Giannelis EP. Macromolecules 1997;30:8000-9.
[13] Nielsen LE. In: Mechanical properties of polymers and composites. New York: Marcel; 1974.
[14] Wang TT, Kwei TK. J Polym Sci A-2 1969;7:889-96.
[15] Fornes TD, Paul DR. Polymer 2003;44:4993-5013.
[16] Privalko VP, Balta Calleja FJ, Sukhorukov DI, Privalko EG, Walter R, Friedrich K. J Mater Sci 1999;34:497-508.
[17] Chow TS. J Mater Sci 1980;15:1873-88.
[18] Nicolais L, Narkis M. Polym Eng Sci 1971;11:194-9.